© 2016 Esteban Lacunza.

CHANNEL-FORMING DISCHARGE AND RIVER MEANDER MIGRATION MODELING OF THE PILCOMAYO RIVER IN THE AREA OF MISIÓN LA PAZ (ARGENTINA) AND POZO HONDO (PARAGUAY)

BY

ESTEBAN LACUNZA

THESIS

Submitted in partial fulfillment of the requirements
for the degree of Master of Science in Civil Engineering
in the Graduate College of the
University of Illinois at Urbana-Champaign, 2016

Urbana, Illinois

Adviser:

Professor Marcelo H. García

Abstract

The Pilcomayo River shows high planform mobility in the area of Misión La Paz (Argentina) - Pozo Hondo (Paraguay) that is associated with the river's bed material and the hydrologic regime of the stream. In order to better understand the river's morphodynamics, RVR Meander, a 2D depth-averaged analytical model, was used to assess the channel's planform evolution in time. The model uses a single discharge value for the simulations, thus estimation of a channel-forming discharge was necessary for the model application.

Of the available methodologies for determining the channel-forming discharge, two are described herein, namely: the bankfull discharge and the effective discharge. The bankfull discharge was obtained with the stage-discharge rating curve after identifying the stage corresponding to the elevation of the active floodplain. The effective discharge was obtained from available data of flow and suspended sediment loads. The results present discrepancy with the bankfull having return periods between 4 and 7 years whereas the effective discharge has 1.01yrs of recurrence interval. Further analysis of the bankfull stage conditions are recommended. The RVR Meander results are compared with river centerline planform variations obtained from LANDSAT imagery for the period between 1987 and 2015. RVR Meander estimations of river mobility were remarkably lower than what the image analysis showed. River channel displacement seems to be caused by the recovery of old meander scars or the occurrence of cutoffs as opposed to bank erosion alone.

To my family.

Table of Contents

List of Tables . . . . . **v**

List of Figures . . . . . **vi**

Chapter 1 Introduction **1**
1.1 Site description 1
1.2 Motivation 3
1.3 Objectives 4

Chapter 2 Methods **6**
2.1 Hydrology 6
2.1.1 La Paz Gaging Station and Compiled Information 8
2.1.2 Hydrologic Statistics 9
2.1.3 Sediment Transport 12
2.2 Channel-forming Discharge 13
2.2.1 Bankfull Discharge (Q_{bf}) 14
2.2.2 Effective Discharge Q_{eff} 16
2.3 River meander migration modeling 19

Chapter 3 Results **24**
3.1 Hydrology 24
3.1.1 Flow Duration Curve 24
3.1.2 Flood Frequency Analysis 26
3.1.3 Flow Measurement Cross Section Hydraulic Properties 27
3.1.4 Sediment Transport 30
3.2 Channel-forming discharge 31
3.2.1 Bankfull Discharge 31
3.2.2 Effective discharge 34
3.2.3 Analysis of the Channel-Forming Discharge Results 36
3.3 River Meander Migration Modeling 38

Chapter 4 Conclusions **43**

References **45**

List of Tables

2.1 Bed material grain sizes of the Pilcomayo River at Misión La Paz. 13

3.1 Statistics of the daily discharge series. 26
3.2 Dicharge values for given return periods using Gumbel's distribution. 26
3.3 Sediment transport annual total load and mean annual load rate. 31
3.4 Flow measurement records with highest water surface stage and maximum water flow rate measured. 32

List of Figures

1.1 Pilcomayo River Basin. 2
2.1 Pilcomayo River Basin at Misión La Paz (Lat: 22° 22' 37.92"S, Long: 62° 31' 23.52"W). 7
2.2 Relationship between water discharge, sediment transport rate, frequency of occurrance, and the product of the frequency and the transport rate (After Andrews (1980)). 17
2.3 Sketch with the definition of the variables used. a) Planform representation. b) Conceptualization of the river cross section (after Motta (2013)). 21
3.1 Mean daily discharge series at La Paz Gaging station from Aug-1961 to Jul-2015. 24
3.2 Monthly discharges of Pilcomayo River at Misión La Paz. 25
3.3 Flow Duration curve in La Paz Gaging station. Data series from Aug 1961 until Jul-2015. 25
3.4 Extreme values analysis using Gumbel's distribution. 26
3.5 Relationship between streamflow and a) Water surface elevation, b)Bed elevation, at La Paz Gaging station. 27
3.6 Relationship between streamflow and cross sectional area in La Paz Gaging station. Data obtained from flow measurement record's in the period between Sep-1972 and Sep-2009. 29
3.7 Relationship between streamflow and cross section mean velocity in La Paz Gaging station. Data obtained from flow measurement records in the period between Sep-1972 and Sep-2009. 29
3.8 Relationship between streamflow and suspended sediment load in La Paz Gaging station. Data obtained from sediment transport measurement record's in the period between Sep-1993 and Aug-2015. 30
3.9 Cross section of the Pilcomayo River located 60m downstream from La Paz gaging station. 32
3.10 Hydraulic reelationships a) Discharge-top width W and hydraulic depth D ratio, b)Discharge- hydraulic depth D ratio, c)Discharge-top width W, d) Top width W - Area A. 33
3.11 Effective discharge computation using 50 class intervals of 91.68 m^3/s each of them. Only sediment grain sizes greater than 62μm were considered. a) Sediment transpor rating curve. b) Water discharge frequency distribution. c) Sediment load frequency distribution. 35
3.12 Comparison of the effective discharge probability to be equaled or exceeded for the Pilcomayo river ar Misión La Paz with data from other sites. 36

3.13 Pilcomayo River paths in the area of Misión La Paz. The river centerlines range between Aug-1987 and Mar-2015. 39
3.14 Results of the migration coefficient calibration. 40
3.15 Results of the river migration during a period of 20yrs. Initial river planform corresponds to Mar-2015. 41
3.16 All river planforms after modeling a period of 20yrs with RVR Meander and natural planforms from 1989-2015. 42

Chapter 1

Introduction

The Pilcomayo River presents one of the highest sediment loads in the world. In the lower part of the basin, the river's planform presents a meandering pattern that flows over an enormous alluvial fan. Historic imagery of the river's planform geometry shows great mobility in time, which might be caused by the fine sands in the river bed as well as the hydrologic characteristics of the river.

Significant advances regarding the understanding and modeling of river meander migration has been made in the past decades. This study characterizes the channel-forming discharge of the river in the region of Misión La Paz and calibrates a 2D analytical model to represent the migration processes. Strengths and limitation of the model are discussed and recommendations for future work are presented.

1.1 Site description

The Pilcomayo River is located in South America and its basin covers a surface of 290,000km^2 approximately (CTRP, 2015), which is shared by Argentina, Bolivia, and Paraguay (see Figure 1.1). The river flows from north west to south east. It is born at the Bolivian Andes mountains and then flows through the *Chaco plains*, a vast flat area which actually is an alluvial fan of great dimensions.

From a social, political, and economical perspective, the Pilcomayo River plays an important role in the region for the following reasons: First, the river's thalweg defines the border between Argentina and Paraguay in the lower basin region; Second, there are

several small towns located near the river banks who use the river as a source of drinking water; Third, the lower part of the river's floodplain is used for agricultural activities which need the river for irrigation purposes.



Figure 1.1: Pilcomayo River Basin. Adapted from CTRP (2015).

The highest part of the watershed reaches elevations above 5,500m whereas the lower altitudes are close to 60m. The Pilcomayo is one of the rivers with highest sediment load rates in the world. An estimation using data available from La Paz gaging station indicates that, on average, it transports 180×10^6tons of sediment annually. The sediments are predominantly generated in the highest part of the basin and then transported downstream.

The river's morphology varies along the stream. A braided pattern is seen in the upper

reaches while a meandering planform is predominant in the lower basin. After flowing out of mountains, the river erodes its own path through the alluvial fan, whose dimensions suggest that the river has changed its path in the past. Today, river meanders show high mobility, specially during the wet season. The suspended sediment load in the lower basin contains material as large as fine sands and as small as clays with a mean grain size corresponding to fine silts. The river bed material presents a slightly coarser composition than the suspended sediment load, with mean grain sizes in the order of fine sands.

The river meanders' high mobility have direct impacts on social, political, and economical aspects. For example, due to the way in which the border between Argentina and Paraguay was established, an abrupt river avulsion could actually change the country in which a town is located. Moreover, certain infrastructure, such as water treatment plants, potable water intakes or irrigation water inlets are difficult to design and build, due to erosion, silting and meander migration processes.

Several infrastructure projects were developed by different governments to mitigate river migration and flooding problems over the years. However, the projects were not coordinated between parties until the creation of a basin management committee in 2000. Since then, several research studies and engineering projects have been developed with the aim of improving the basin's inhabitants quality of life as well as of ensuring the water resource sustainability.

1.2 Motivation

River meandering has been subject of research for more than a century (e.g., Thomson, 1876; Davis, 1908). Since then, great advances were made in the study of river meander migration processes such as the river hydrodynamics, sediment transport, river bed morphodynamics, and bank erosion mechanisms. During the last decades, several authors have been working on the development of tools to represent both the hydrodynamics an morphology of the river

(e.g., Ikeda, Parker, & Sawai, 1981; Johannesson & Parker, 1989; Zolezzi & Seminara, 2001). This knowledge has been applied in the field of water resources engineering for the analysis of river training structures, river restoration processes and improved their development. Models such as the RVR Meander software, developed by Abad and García (2006) can be used to assess the prediction of the migration of river meanders. In general, this kind of models present some limitation such as considering constant channel width, and simplified representation of secondary flows in channel bends. Nevertheless, they represent a useful tool for engineering purposes.

In the case of the Pilcomayo River, it presents high planform geometry mobility and several problems have occurred due to erosion processes near populated areas or infrastructure. The understanding of the sediment transport and its relation to the morphodynamics of the river combined with the use of models such as RVR Meander, are useful tools to assess the river's planform evolution in time.

The purpose of this study was to estimate the channel-forming discharge that characterizes the river channel geometry and to estimate the river meanders migration by the use of the RVR Meander software.

1.3 Objectives

The general objective of this study was to estimate the channel-forming discharge of the Pilcomayo River in the area of Misión La Paz and to model the river's planform evolution using a 2D analytical model under such conditions.

The specific objectives are:

1. Characterize the river water discharge regime, sediment transport, and river channel properties in the area of Misión La Paz, Salta, Argentina.

2. Estimate the channel-forming discharge of the Pilcomayo River in the region of Misión La Paz .

3. Set up the *RVR Meander* river meander migration model to represent the Pilcomayo River behavior and calibrate it using river past conditions obtained from LANDSAT images.

4. Simulate the Pilcomayo River with predefined scenarios in order to predict the river meander migration and its planform evolution and discuss the limitations of the model used and methodology applied in the study..

Chapter 2

Methods

A thorough description of the methods applied for this study is presented herein. The chapter is divided in four sections. First, the methodology used to describe the river hydrology is summarized. Second, a discussion of the available methods for computing the channel-forming discharge is given including the reasons for choosing the methodology used in this study. In the third section, the approach used to characterize the river planform geometry using satellite images is presented. Finally, the RVR Meander software is described as well as the methodology used to define the input parameters required to run the model.

2.1 Hydrology

The present study analyzes the Pilcomayo River hydrology in the area of Misión La Paz, Salta, Argentina. The whole river basin spans an area of 290,000km^2 but down to Misión La Paz the areal extent of the basin covers 90,802km^2, as shown in Figure 2.1. The elevations displayed in the figure were obtained from 3-arc-second SRTM images (USGS, 2012) which correspond to approximately 90x90m grid cells. The basin's boundary as well as the river path were defined using the Hydrology package of the Spatial Analyst toolbox of ArcGis®.

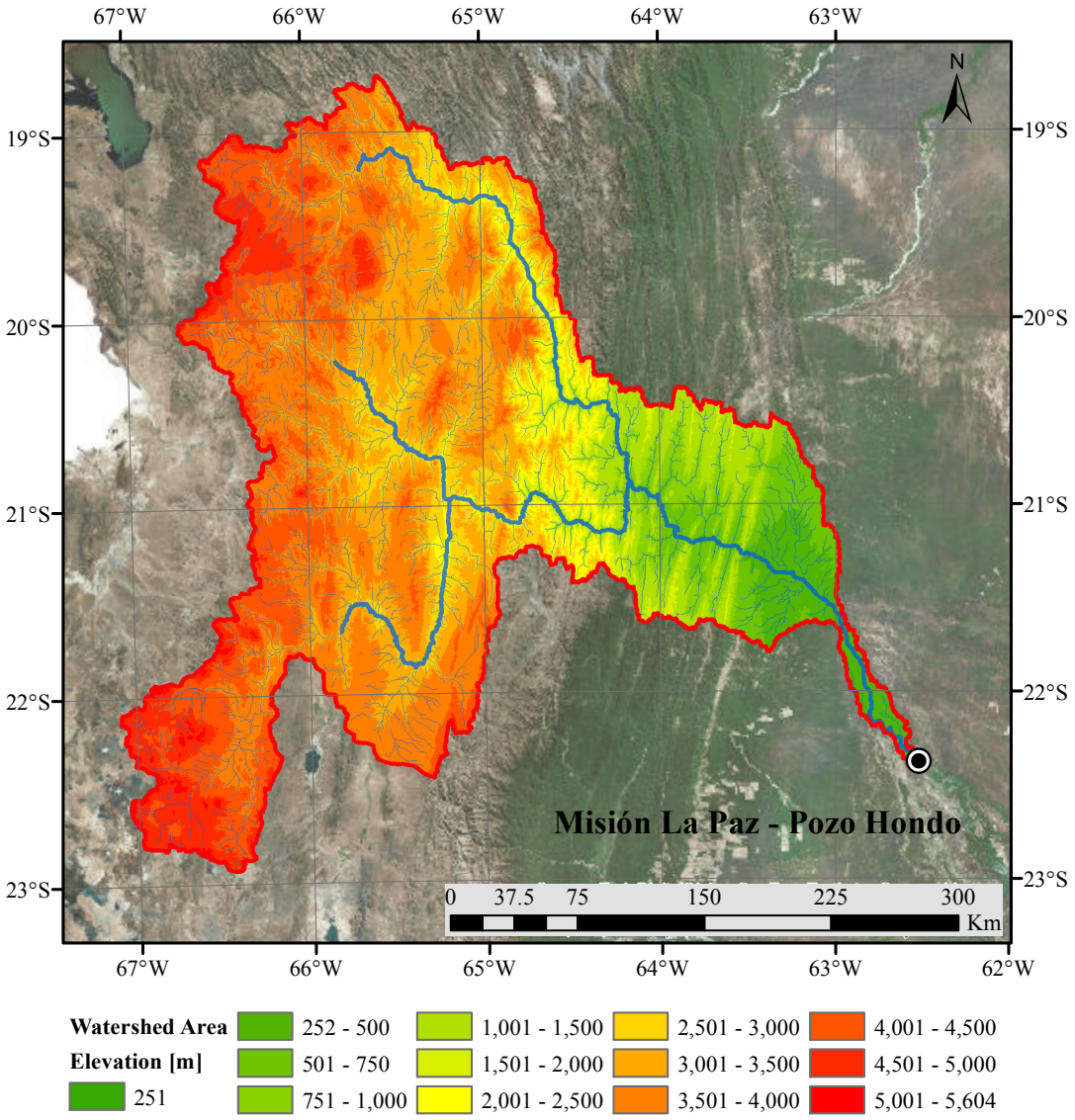


Figure 2.1: Pilcomayo River Basin at Misión La Paz (Lat: 22° 22' 37.92"S, Long: 62° 31' 23.52"W). Topographic and elevation data were obtained from SRTM images (USGS, 2012).

The basin hydrology presents a strong seasonality dividing the hydrologic year between the wet season, between November and April, and the dry season, between May and October. The main stream water source is the precipitation runoff that falls in the highest part of the basin in the Bolivian Andes.

2.1.1 La Paz Gaging Station and Compiled Information

"La Paz" gaging station is located 500m upstream of the international bridge that was built between the towns of Misión La Paz, Argentina, and Pozo Hondo, Paraguay. Its coordinates are Lat: 22° 22' 37.92"S and Long: 62° 31' 23.52"W. At this location, the river acts as the border between both countries, with the left bank being Paraguayan and the right bank Argentinian. The gaging station was installed in the 1940s but began to operate continuously after 1961. This station is managed by the Argentinian National Water Resources Under Secretary, and hydrometric data is available on their website (see SSRH (2015)).

The following information was obtained from this source:

- Daily mean stage values from Sep-1964 to Jul-2015.
- Daily mean flow values from Aug-1961 to Jul-2015. This series is the result of applying the rating curve equation to the stage reading. It is important to mention that during the last decade the rating curve equation changed every hydrological year due to the river channel's geometry variations produced by floods.
- Suspended sediment concentration values between Sep-1993 and Aug-2015.

The Pilcomayo Basin Committee also provides access to La Paz station hydrometry data on their website (CTRP, 2015). Additional information was obtained directly from this source and other sets of data were facilitated by Committee staff via email communication. The information obtained is described below:

- A total of 8,392 flow measurements conducted between Sep-1972 and Feb-2015. This dataset includes the date of the measurement, flowrate computed, gage reading, mean velocity, and flow area.
- Detailed information of more than 2,500 streamflow measurements conducted between 1984 and 2015. The data includes cross section's profile surveyed during

discharge measurements, cross sectional area, mean velocity and gage stage during measurements.

- Topographic and bathimetric surveys conducted in 2008, 2011, and 2014.

Historically, the flow measurements were taken at the same site where the gaging station is located. However, the measurement cableway was destroyed during a flood in 2009. Although the stream gage remained at the same place, the flow measurement cross section was relocated 850m downstream of the gage, and 350m downstream of the bridge. Consequently, the flow measurements taken after 11-30-2009 do not correspond to the place where the gage is located. Only discharge values and gage readings can be used from flow measurement data after the cableway was relocated. The flow areas, velocities, and other information cannot be compared with measurements taken before 11-30-2009.

2.1.2 Hydrologic Statistics

The compiled information served as input for the computation of hydrological predictors and parameters describing the watershed characteristics and stream behavior. Depending on the purpose and use of the parameters computed, different input data sets were selected. The following sections describe the parameters computed and the input information used.

Flow Duration Curve

The flow duration curve represents the probability of an event to be equaled or exceeded. To build the curve, the discharge values were ranked and the probability of exceedance was calculated using Weibull's expression.

$$P\left(Q \geq Q_m\right) = \frac{m}{n+1} \tag{2.1}$$

Where m is the value's ranking and n the total number of values. Data used corresponds with the mean daily discharge values from Aug-1961 to Jul-2015.

Flood Frequency Analysis

The series of daily annual maxima was used for the computation of extreme flow values. This means that the maximum discharge value of each hydrological year was selected. The data series analyzed corresponds to the mean discharge values between Aug-1961 and Jul-2015. Hence, a new series of 54 flow rate values was obtained. A Gumbel distribution function was selected for fitting the data. The cumulative frequency distribution is,

$$F(x) = Prob\,(x \leq x_T) = \exp\left[-\exp\left(-y\right)\right] \tag{2.2}$$

$$y = \alpha\,(x_T - u) \tag{2.3}$$

Where,

$$\alpha = \frac{\sigma_N}{\sigma} \tag{2.4}$$

$$u = \mu - \frac{y_N}{\alpha} = \mu - \frac{y_N}{\sigma_N}\sigma \tag{2.5}$$

In this expression, μ is the mean value of the data set, σ is the standard deviation, and y_N and σ_N are coefficients that depend on the length of the data set (Gumbel, 1958, p.228). For 54 values, $y_N = 0.5501$ and $\sigma_N = 1.1667$. Calling T the return period,

$$\frac{1}{T} = p = Prob\,(x \geq x_T) \tag{2.6}$$

Therefore,

$$F(x) = Prob\,(x \leq x_T) = 1 - Prob\,(x \geq x_T) = 1 - \frac{1}{T} \tag{2.7}$$

Merging (2.2) with (2.7) and solving for x_T,

$$\exp\left[-\exp\left(-y\right)\right] = \exp\left\{-\exp\left[-\alpha\left(x_T - u\right)\right]\right\} = 1 - \frac{1}{T} \tag{2.8}$$

$$\alpha\left(x_T - u\right) = -\ln\left[\ln\left(\frac{T-1}{T}\right)\right] \tag{2.9}$$

$$x_T = u - \frac{1}{\alpha}\ln\left[\ln\left(\frac{T-1}{T}\right)\right] \tag{2.10}$$

$$x_T = \mu + \sigma\left\{\frac{-\ln\left[\ln\left(\frac{T-1}{T}\right)\right] - y_N}{\sigma_N}\right\} \tag{2.11}$$

$$x_T = \mu + \sigma\kappa_T \tag{2.12}$$

Where κ_T, known as the frequency factor, is independent of the mean and standard deviation values. It only depends on the selected return period and the length of the data series.

The confidence intervals are computed with the following expressions (Chow, 1988), which represent the upper U_{lim}, and lower L_{lim} limits.

$$U_{lim} = x_T + s_e \times z_\alpha \tag{2.13}$$

$$L_{lim} = x_T - s_e \times z_\alpha \tag{2.14}$$

$$s_e = \left[\frac{1}{n}\left(1 + 1.396\kappa_T + 1.1\kappa_T^2\right)\right]^{1/2}\sigma \tag{2.15}$$

Where n is the number of elements of the series, and z_α is the normal standard variable with an exceedance probability value of α. In this case, a significance level of $\alpha = 0.05$ was chosen and consequently $z_\alpha = 1.645$. This corresponds to a confidence level β of 90%, since $\alpha = \frac{1-\beta}{2}$.

Flow Measurement Cross Section Hydraulic Properties

The flow measurements data set, together with the detailed reports data series, were used to relate different hydraulic parameters at the cross section used for measurements. A set of variables such as cross sectional area, mean velocity, top width, hydraulic depth, water surface elevation, river bed elevation, and wetted perimeter were plotted against water discharge. Analytical functions were then obtained by fitting power curves using the least squares method.

2.1.3 Sediment Transport

Data of suspended sediment load at La Paz station is available since September 1993 (SSRH, 2015). According to Martín-Vide, Amarilla, and Zárate (2014), the samples were obtained using a depth integrating sampler at three different verticals in the cross section. the samples are then processed in the laboratory and the material was divided between fine and coarse using a 62μm mesh as the threshold. No data regarding bedload material was found. However, Martín-Vide et al. (2014) state that suspended load was the most significant transport mechanism in the Pilcomayo River.

Particles size distributions of suspended load samples were reported by Orfeo (2007). According to the author, the analysis of 15 samples taken between Dec-2006 and Mar-2011 present average sand, silt, and clay contents of 34%, 41%, and 25% respectively.

In his study, Orfeo also analyzed samples taken from the river bed. As expected, the bed material is coarser than the material in suspension, with sand contents dominating over finer grains. Specifically, he found distributions with 88% sand, 8% silt, and 4% clay on average. The author also reported grain size distribution analysis of the bed material for samples taken on four different days between Dec-2006 and Nov-2007. Although Orfeo conducted sample analysis at three different vertical locations for each survey, only average values of the cross section are reported for each day. Table 2.1 shows a summary of D_{10}, D_{50}, and

D_{90} where the subscripts represent the percentage of finer material in the sample.

Table 2.1: Bed material grain sizes of the Pilcomayo River at Misión La Paz.

Date	Gage reading [m]	Discharge [m^3/s]	D_{10} [mm]	D_{50} [mm]	D_{90} [mm]
12/20/2006	3.13	139	0.084	0.149	0.238
2/27/2007	3.06	232.4	0.092	0.165	0.244
8/14/2007	2.6	23.6	0.083	0.144	0.233
11/1/2007	2.43	8	0.083	0.144	0.234
Average			0.085	0.151	0.237

The table shows that mean grain sizes are in the range of fine sands and the content of fine material is less than 10% since all D_{10} values reported are above the 62μm threshold.

2.2 Channel-forming Discharge

The channel form of a river can be thought of as the consequence of the interaction of a number of interdependent variables such as streamflow watershed topography, geology, soil properties, vegetation, climate, etc. However, their effect on channel form can be described by the discharge and the sediment load, which are dominant factors that integrate all the others Knighton (1998).

The channel-forming discharge is a theoretical concept from geomorphology that argues that if a certain stream flow is maintained constant in time, the stream would develop the same channel shape and morphology as the natural river bankfull characteristics generated by actual hydrologic fluctuations. Similar definitions can be found in the literature under the name of *channel-forming* or *dominant* discharge (e.g., Inglis & Lacey, 1947; Ackers & Charlton, 1970; Dunne & Leopold, 1978; Knighton, 1998; Biedenharn, Copeland, Thorne, Soar, & Hey, 2000; Soar & Thorne, 2001).

Variations in river hydrology impact the channel's geometry, which may be modified depending on the magnitude of the hydrologic event and on bed material properties as well. The concept of channel-forming discharge implies that in longer periods of time the

stream would tend to adjust and return to a quasi-equilibrium state (Soar & Thorne, 2001; Biedenharn, Watson, & Thorne, 2008). However, Biedenharn et al. (2008) also claim that the climate and hydrological variability of the river basin play an important role in the river's recovery after major events. According to the authors, perennial streams recover faster than ephemeral rivers, specially those found in semi-arid regions. Furthermore, it has been suggested that the applicability of the channel-forming discharge may be questioned (Soar & Thorne, 2013). This situation may be the case of the Pilcomayo River, since it presents a strong hydrologic seasonality. However, it is necessary to perform the estimations and check the results with real cases in order to be certain about the applicability of this channel-forming concept.

Since the dominant discharge is a theoretical concept, no true methodology exists to compute it. Nevertheless, some different morphological criteria such as the bankfull or the effective discharges have been discussed in the literature to be representative of the channel-forming discharge. Although some authors (e.g., Andrews, 1980; Carling, 1988) found that bankfull and effective discharges are equivalent in some types of river, this is not a general rule. Other authors found discrepancies between the results of both concepts (e.g., Benson & Thomas, 1966; Sholtes & Bledsoe, 2016).

2.2.1 Bankfull Discharge (Q_{bf})

The bankfull condition refers to the situation in which the main river channel is completely full, but there is no spill of water into the floodplain. Similar definitions have also been presented by Nixon (1959); Wolman and Miller (1960); Leopold, Wolman, and Miller (1964); Williams (1978); Biedenharn et al. (2000); Soar and Thorne (2001).

Although there is general agreement regarding the bankfull concept, no clear procedure has been developed to determine its location within the cross section. Several criteria may be found in the literature from which different bankfull values may result, increasing the uncertainty (Harman, Stewardson, & DeRose, 2008; Johnson & Heil, 1996).

Williams (1978) summarizes ten different procedures available in the literature for determining the bankfull stage. Some of these methods require the identification of sedimentary surfaces such as the elevation of the active flood plain, the location of the low benches or the elevation of the channel bars' higher surface. Another group of methodologies requires the identification of boundary features such as the line of perennial vegetation. Finally the author describes a third group that computes the bankfull stage from measured cross sections. Once the bankfull stage is obtained, the corresponding discharge may be determined using a rating curve, or relations such as Chezy or Manning.

Hydraulic geometry of the cross section can also be used to determine the bankfull discharge. For example, Wolman (1955) defines the bankfull stage as the elevation that minimizes the ratio between the top width and the water depth. Other relations can be analyzed such as discharge and flow area, discharge and width or discharge and water depth. A slope change in the relation between the variables can be indicative of the bankfull condition.

A frequency of occurrence criteria has been used by other authors. For example, Leopold et al. (1964) argues that Q_{bf} has a return period between 1 and 2 years, Nixon (1959) found that in England the probability of exceedance of the bankfull discharge is in the order of 60%. Similarly, (Andrews, 1980) found bankfull frequencies in the range of 1.18 and 3.26 years. However, other researchers argue that in some cases the bankfull discharge can present return periods as high as 32 years (Williams, 1978).

For the purpose of this study, bankfull discharge is determined using the hydraulic properties of the cross section where the cableway for flow measuremnts at La Paz gaging station was located until 2009. Data used corresponds to the period between 1984 and 2009. The data set includes mean flow areas (A), mean flow velocities (U), and surveyed cross section topography. This bathimetry was used to compute the top width (W), water depth (y), wetted perimeter (P), hydraulic depth(D), and hydraulic radius (R_h). Then, geometric relations such as Qvs$A$, Qvs$W$, Avs$W$, and QvsW/D were plotted and analyzed

in order to identify the bankfull discharge and elevation. A cross section survey, covering part of the floodplain, was obtained from (CTRP, 2015). The survey was conducted in Aug-2014 and the cross section measured is located downstream of the gage station at a distance of approximately 60m. This information helps to visually define the floodplain stages and to contrast this information with the results of the hydraulic properties analysis. In addition, the flood frequency analysis conducted with data from the same hydraulic section was used to estimate a possible range for the bankfull discharge based on the frequencies presented by different authors.

2.2.2 Effective Discharge Q_{eff}

First introduced by Schaffernak (1922), the effective discharge is defined as the water streamflow that transports the largest annual amount of sediment over a period of years (Andrews, 1980). This concept considers that in addition to the magnitude of the events, their frequency also plays an important role in establishing the channel's geometry.

Large hydrologic events have more power to erode and to modify the channel's geometry in short periods of time. However, their frequency of occurrence is low, so their role in sediment transport in longer periods of time is reduced. In contrast, smaller events but with higher frequencies were found to be the main reason responsible for annual sediment loads in alluvial rivers (Gandolfo, 1940; Wolman & Miller, 1960).

When analyzing the similarities between bankfull and effective discharges, Soar and Thorne (2001) argue that they are equivalent and this is explained from an energy balance point of view. For long periods of time, the river tends to minimize the energy used in the water conveyance and this situation is reached for both the effective discharge and when the channel is full but without spilling over into the floodplain.

Some authors (e.g., Andrews, 1980; Carling, 1988) found agreement between bankfull and effective discharge values in several streams. However, Soar and Thorne (2013) found that in average the effective discharge is 14% lower than the Q_{bf}. In addition, Biedenharn

et al. (2008) remark that bankfull and effective discharge are not always the same and that Q_{eff} may not be suitable for estimating dominant discharges in all cases.

The general methodology for computing Q_{eff} consists in determining the sediment load and frequencies of occurrence for water discharge classes, and then multiplying both of them. The effective discharge is selected as the point that shows the maximum value on the resulting curve. Figure 2.2 presents a conceptual scheme of the procedure.

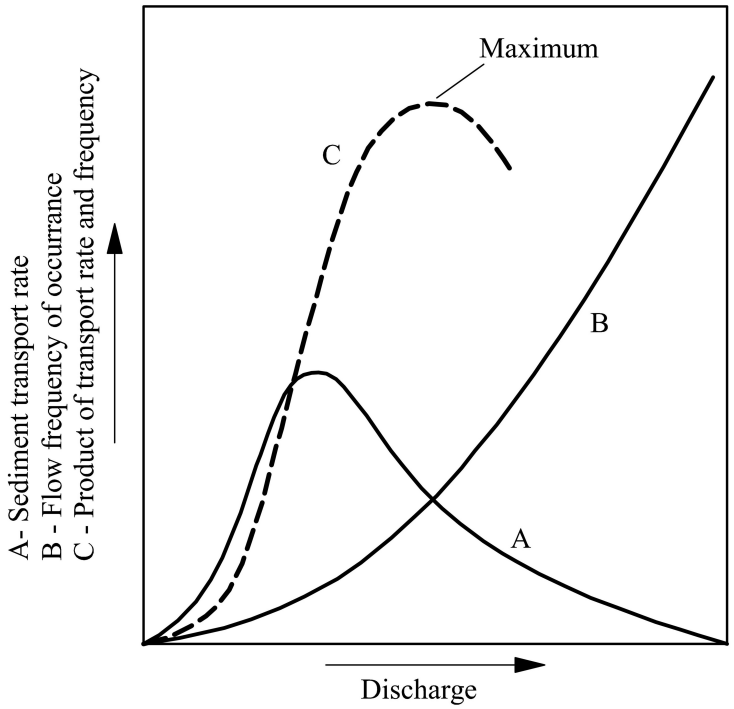


Figure 2.2: Relationship between water discharge, sediment transport rate, frequency of occurrance, and the product of the frequency and the transport rate (After Andrews (1980)).

Different procedures can be found in the literature regarding the process to determine the effective discharge. For example, Biedenharn et al. (2000) and Soar and Thorne (2001) opt for constructing frequency histograms while Nash (1994) prefers to fit a distribution function to the data. The advantage of the latter method is that analytical functions show smoother results than the former approach which may present multiple peaks or have irregular shapes. However, it is possible that the fitting curve has no good correlation so the results can be biased by this fact.

For the purpose of this study, the procedure suggested by Biedenharn et al. (2000, 2008) and Soar and Thorne (2001) was selected. This methodology requires the flow duration curve and the sediment transport rating curve as inputs.

The following data was selected for the analysis.

- *Flow duration curve*: Daily mean flow data values from Aug-1961 to Jul-2015.
- *Sediment transport rating curve*: Although this curve should include bedload and suspended load as well, no bedload data is available. However, (Martín-Vide et al., 2014) suggest that the bedload represents less than the 12% of the total sediment load. In addition, only the coarser grain sizes ($\geq 62\mu$m) were taken into account since the finer part is considered wash-load, which does not interact with the river bed. The rating curve for the coarse portion of the material in suspension is presented in the section pertaining sediment transport.

The first step in the procedure is to construct the histogram of flow frequencies, which was computed using the flow duration curve. This curve represents the cumulative distribution function of the exceedance probability. Then, the frequency of each interval in the histogram corresponds with the difference between the cumulative probability of the interval limits.

An important step is the definition of the number of classes for the histogram. Although there is no precise rule for its definition, there is general agreement that the number should be between 10 and 25 (Biedenharn et al., 2000). However, the authors suggest that higher numbers may be used in the case of high hydrologic variability. According to Soar and Thorne (2001), if the intervals are too big, the histogram would not represent properly the frequency distribution. On the other hand, the author indicates that too small intervals may not produce a continuous distribution or lead to intervals with zero frequency.

For base flow dominated streams, where the frequency distribution presents a strong positive skewness, some considerations have to be made. In these cases, it is highly probable that the effective discharge will be represented by the first segment. The use of logarithmic

intervals instead of arithmetic (Nash, 1994) solves this issue. However, (Soar & Thorne, 2001) demonstrated that using logarithmic intervals biases the resulting effective discharge, and overestimates it. When the effective discharge falls in the first class, Biedenharn et al. (2000) recommend to increase the interval size to better define the frequency distribution.

Once the number of intervals is chosen, their size is computed by dividing the difference between the maximum and minimum discharges in the flow duration curve by the number of classes. the lower limit of the first class corresponds with the minimum discharge and its upper limit is determined by adding to it the interval size. At this point, the second interval begins, and the process is repeated until the highest discharge value is reached.

The following step uses the sediment transport rating curve to compute the sediment load rates that correspond to the mean flow in each interval. Finally, the weighed contribution of sediment load and flow duration corresponding to each class interval is obtained by multiplying the intervals' sediment load and the corresponding frequency. The resulting histogram should present a continuous shape with a single mode. If this is the case, the effective discharge corresponds to the water flow that shows the highest value.

2.3 River meander migration modeling

River meander migration is the consequence of instabilities generated by complex processes that can be represented by the river hydrodynamics, the sediment transport, the bed mophodynamics, and the bank erosion mechanisms. The role of the hydrodynamics is to represent the water flow characteristics and the stresses generated on the water-bed interface. These stresses reduce the stability of the bed material which may start to move under certain conditions. The bed morphodynamics studies the bed shape patterns and its evolution in time. Finally, river migration is due to the erosion and sedimentation processes of the banks. These processes are deeply related to the floodplain's morphological and ecological characteristics. All mentioned processes interact with each

other and this is the main reason for the complexity of river migration processes.

The RVR Meander software was developed with the purpose of aiding in the evaluation of river restoration and re-naturalization projects of alluvial streams. It was developed by Abad and García (2006) and first introduced in 2006. The software provides two different modules. The first one is used to conduct a statistical analysis of the river's planform characteristics such as sinuosity, skewness, and rate of migration. Then, the second module holds the river migration code for modeling the river meander centerline migration.

Conceptually, the river migration code presents three parts. First, the code models the hydrodynamics of the river, and with these results, the bank erosion and the bank displacement are computed. Finally, a third part computes the migration of the river centerline. It is beyond the scope of this study to make a thorough analysis of the theory and numerical aspects of the the model. Nevertheless, basic guidelines on the concepts and assumptions behind the the RVR Meander model are discussed.

RVR Meander's hydrodynamic model represents the river stream with a 2D depth-averaged analytical model based on Ikeda et al. (1981) work. In its derivation, the model makes the assumption of quasi-steady flow conditions. This means that morphologic processes occur in time scales much longer than the hydrodynamic ones. In addition, the model assumes a constant channel width along the stream.

The equations of motion for the meandering channel used in the model are expressed in intrinsic coordinates, where s^* corresponds to the streamwise, and n^* to the normal components.

$$\frac{1}{1+n^*C^*}U^*\frac{\partial U^*}{\partial s^*}+V^*\frac{\partial U^*}{\partial n^*}+\frac{C^*}{1+n^*C^*}U^*V^*=-\frac{g}{1+n^*C^*}\frac{\partial H^*}{\partial s^*}-\frac{\tau_s^*}{\rho D^*} \tag{2.16}$$

$$\frac{1}{1+n^*C^*}U^*\frac{\partial V^*}{\partial s^*}+V^*\frac{\partial V^*}{\partial n^*}-\frac{C^*}{1+n^*C^*}U^{*2}=-g\frac{\partial H^*}{\partial n^*}-\frac{\tau_n^*}{\rho D^*} \tag{2.17}$$

$$\frac{1}{1+n^*C^*}\frac{\partial\left(U^*D^*\right)}{\partial s^*}+\frac{\partial\left(V^*D^*\right)}{\partial n^*}+\frac{C^*}{1+n^*C^*}V^*D^*=0 \tag{2.18}$$

Dimensionless variables are indicated without the star $(*)$. Depth-averaged velocities in s^* and n^* are expressed by U^* and V^* respectively. H^* holds for the water stage whereas $D*$ is the water depth and η is the bed elevation. τ_s^* and τ_n^* are the shear stresses in the streamwise and normal direction, g is the acceleration of gravity, and ρ is the water density. Time is represented by t^*, the bed porosity by λ_p and the bed load transport rates in s^* and n^* are q_s^* and q_n^* respectively. Other variables are the channel half-width B^* and the local curvature C^*. A sketch of the conceptual model of the river with the definition of the main variables is presented in Figure 2.3.

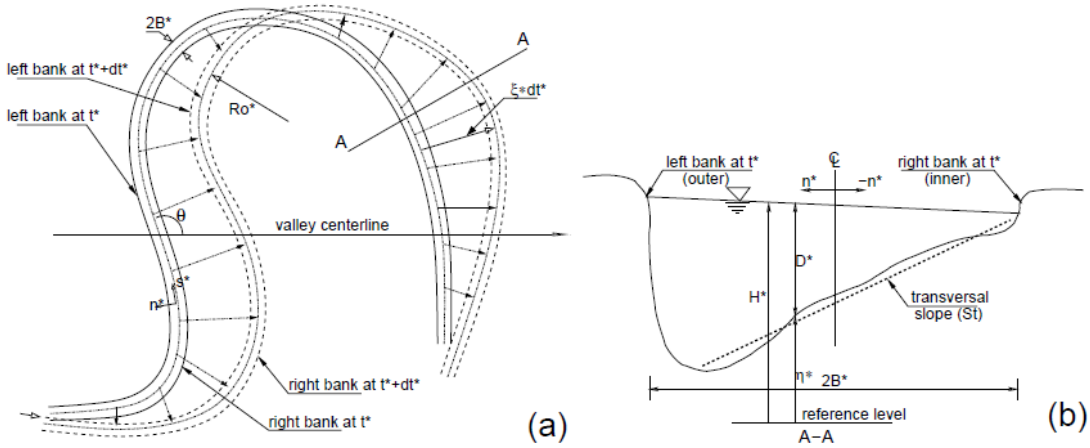


Figure 2.3: Sketch with the definition of the variables used. a) Planform representation. b) Conceptualization of the river cross section (after Motta (2013)).

The bed shear stress vector is computed as:

$$\tau^* = (\tau_s^*, \tau_n^*) = \rho C_f \sqrt{U^{*2} + V^{*2}} \, (U^*, V^*) \, . \tag{2.19}$$

Where C_f is the friction coefficient.

The equations are linearized assuming a small perturbation in the channel centerline, which means that the radius of curvature is much smaller than the half-width. Hence, the variables are expressed as a mean value plus a fluctuation. Details of this procedure can be seen in Motta (2013). A scour factor A is introduced in the equations to take into account the transverse slope of the channel due to secondary flows. In addition, a bank erosion model is incorporated, which relates the near-bend velocities to bank migration. Consequently, the relation $\zeta = E_o U$ is assumed, where ζ is the total erosion and E_o is the erosion or migration coefficient. Another model of bank erosion was introduced later by Motta (2013), which is based on physical characteristics of the margins and floodplains. However, in this study, the migration coefficient model is applied. Apart from the bank erosion model, RVR Meander enables another mechanism of bank displacement by enabling neck cutoffs to occur along the stream when two bends approximate each other less than a certain threshold distance defined by the user. This constant value corresponds to a number of channel half-widths. It is important to remark that other mechanisms such as chute cutoffs, avulsions, or recapturing of meander scars are not included in this model.

Input data required by the model includes the initial river planform geometry, and the valley centerline. For this purpose, digitized river paths obtained from LANDSAT images (USGS, 2012) in the period between 1987 and 2015 were used. Then, the properties of the channel geometry as well as hydraulic parameters are required. For this analysis, the effective discharge computed in the channel-forming discharge section was used. In addition, hydraulic relations found in the analysis of the bankfull discharge were used to select the channel width.

The valley slope, the bed material properties and the Manning's coefficient are also

required for the hydrodynamic computations. According to topographical surveys from CTRP (2015), and in accordance with the values obtained by Barbagelata (2010), the valley slope in the region of Misión La Paz is on the order of 0.0003-0.0004. Hence, a value of 0.00035 was used. The bed material grain sizes were already analyzed in the sediment transport methods section. A mean grain size of $D_s = 0.15$mm was selected.

The scour factor relates the channel transverse slope with the the curvature at the bend and the channel's width. Different values for the scour factor have been presented in the literature. Zimmerman and Kennedy (1978) found values between 1.6 and 8.8 from laboratory data, using a circular flume. Later, Odgaard (1981) found values between 3 and 8 approximately from lab and field data. Furthermore, Garcia, Bittner, and Nino (1994) suggests that the scour factor ranges between 3 and 10. In the analysis of the Pilcomayo River, a value of $A = 4$ was selected.

The first step for the modeling process is to calibrate the model. Specifically, the migration coefficient is adjusted by modeling the river's planform evolution in short periods of time (usually 5 years long) and comparing the results with the available satellite imagery. The images selected for the calibration used the period from Aug-1987 to Dec-1992.

The main objective of the modeling effort is to determine an envelope of river planform locations over a period of 20 years starting from different channel centerlines. This envelope may indicate the possible locations of the river path in the future. The set of initial river centerline conditions were defined by the river paths digitized from the LANDSAT images.

Chapter 3

Results

3.1 Hydrology

The results of the hydrologic analysis of the Pilcomayo River at Misión La Paz is presented herein. The daily mean discharge series from August 1961 to July 2015 is presented in Figure 3.1. The data series shows 54 peaks that correspond to the wet season of each hydrological year. The basin presents a strong seasonality, with higher water discharges between November and April, and low water flows between May and October.

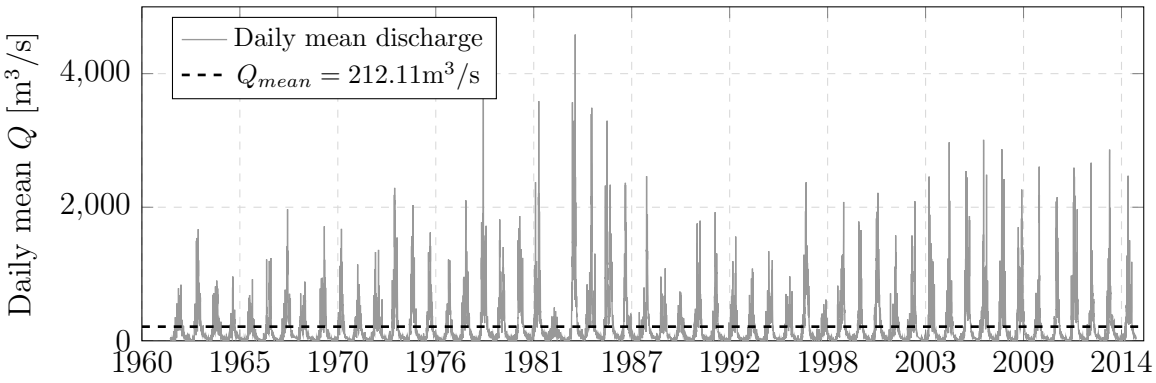


Figure 3.1: Mean daily discharge series at La Paz Gaging station from Aug-1961 to Jul-2015.

3.1.1 Flow Duration Curve

The seasonal fluctuations of the streamflow can be seen in Figure 3.2. Monthly minimum, mean, median, and maximum values are presented. February shows higher water discharges on average.

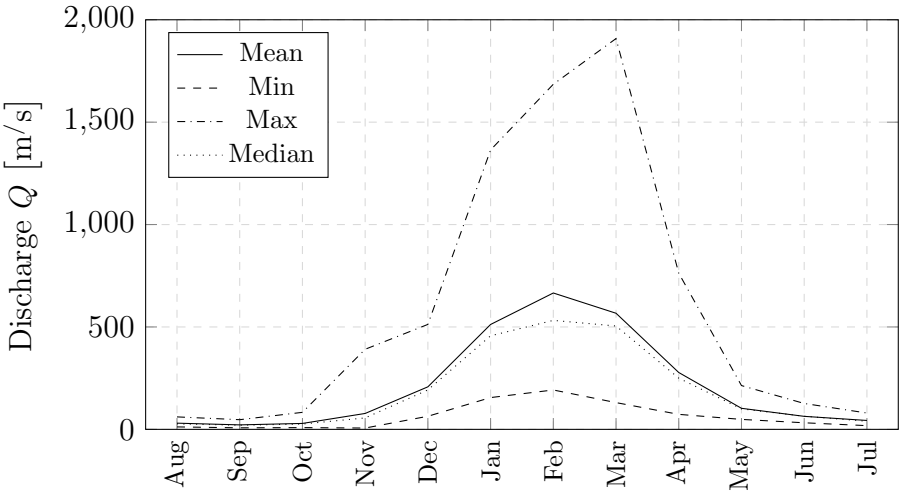


Figure 3.2: Monthly discharges of Pilcomayo River at Misión La Paz.

The flow duration curve for the daily stream flow series is shown in Figure 3.3. In addition, the stream flow values for different percentiles are shown in table 3.1. It is worth noting that the duration that corresponds to the mean annual daily discharge is approximately 27.8%. This means that the frequency distribution has a positive skewness.

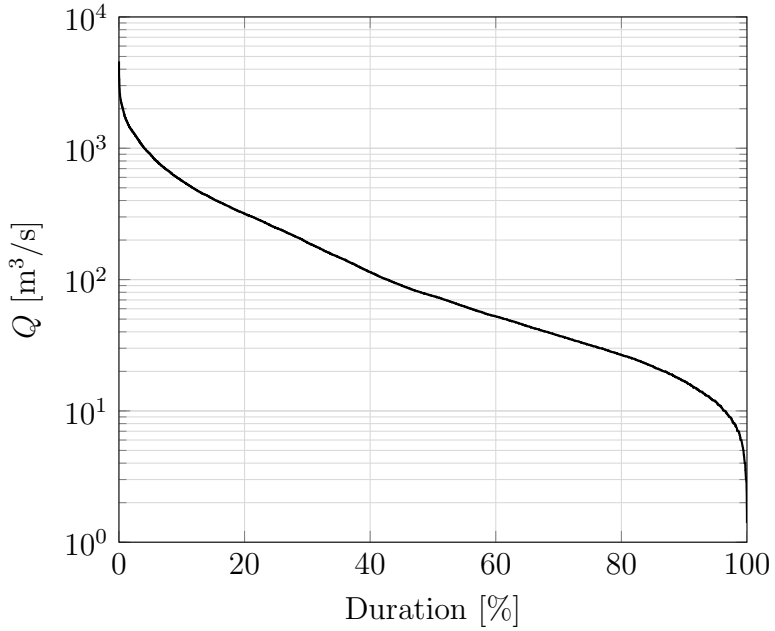


Figure 3.3: Flow Duration curve in La Paz Gaging station. Data series from Aug 1961 until Jul-2015.

Table 3.1: Statistics of the daily discharge series.

D [%]	Q_{max}	1	5	10	25	50	75	90	95	99	Q_{min}	Q_{mean}
Q_w[m^3/s]	4585	1716	892	562	245	74	31	16	11	5	1	212

3.1.2 Flood Frequency Analysis

The results of the flood frequency analysis using the annual daily maxima flow series between Aug-1961 and Jul-2015 are presented in Figure 3.4. The parameters computed to construct Gumbel's distribution are $\mu = 1981.64$m^3/s, and $\sigma = 875.153$m^3/s. It can be seen that all points are located within the confidence intervals. The obtained flow rates for increasing return periods are presented in table 3.2.

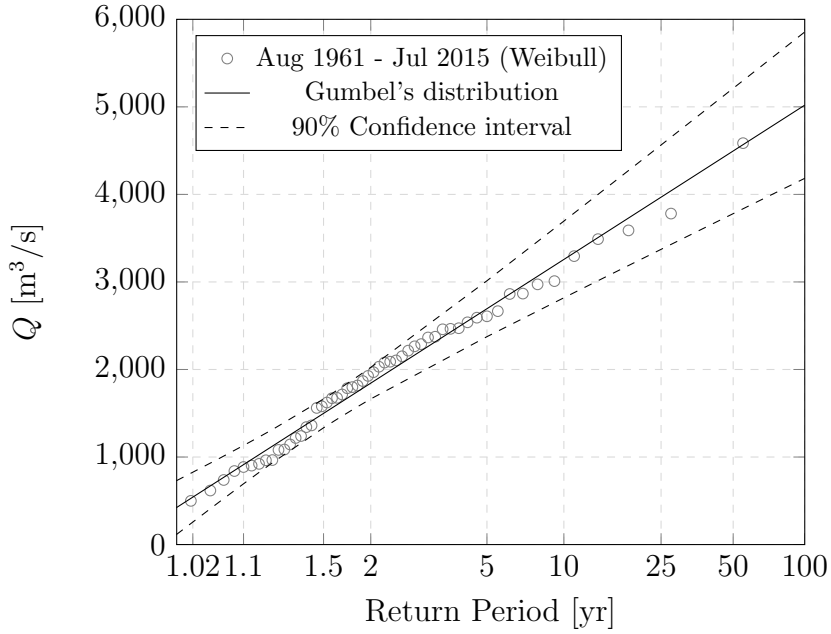


Figure 3.4: Extreme values analysis using Gumbel's distribution.

Table 3.2: Dicharge values for given return periods using Gumbel's distribution.

Return period [yr]	1.01	1.1	1.5	2.33	5	10	25	50	100
Discharge [m^3/s]	422	913	1498	2003	2694	3257	3968	4496	5020

3.1.3 Flow Measurement Cross Section Hydraulic Properties

Some of the hydraulic properties relations obtained, such as $Q-Width/Depth$ and $A-W$ are discussed later in the bankfull discharge section. Here, the focus is on the relation between the discharge, the water surface elevation, and the river bed elevation. These variables are plotted in Figure 3.5.

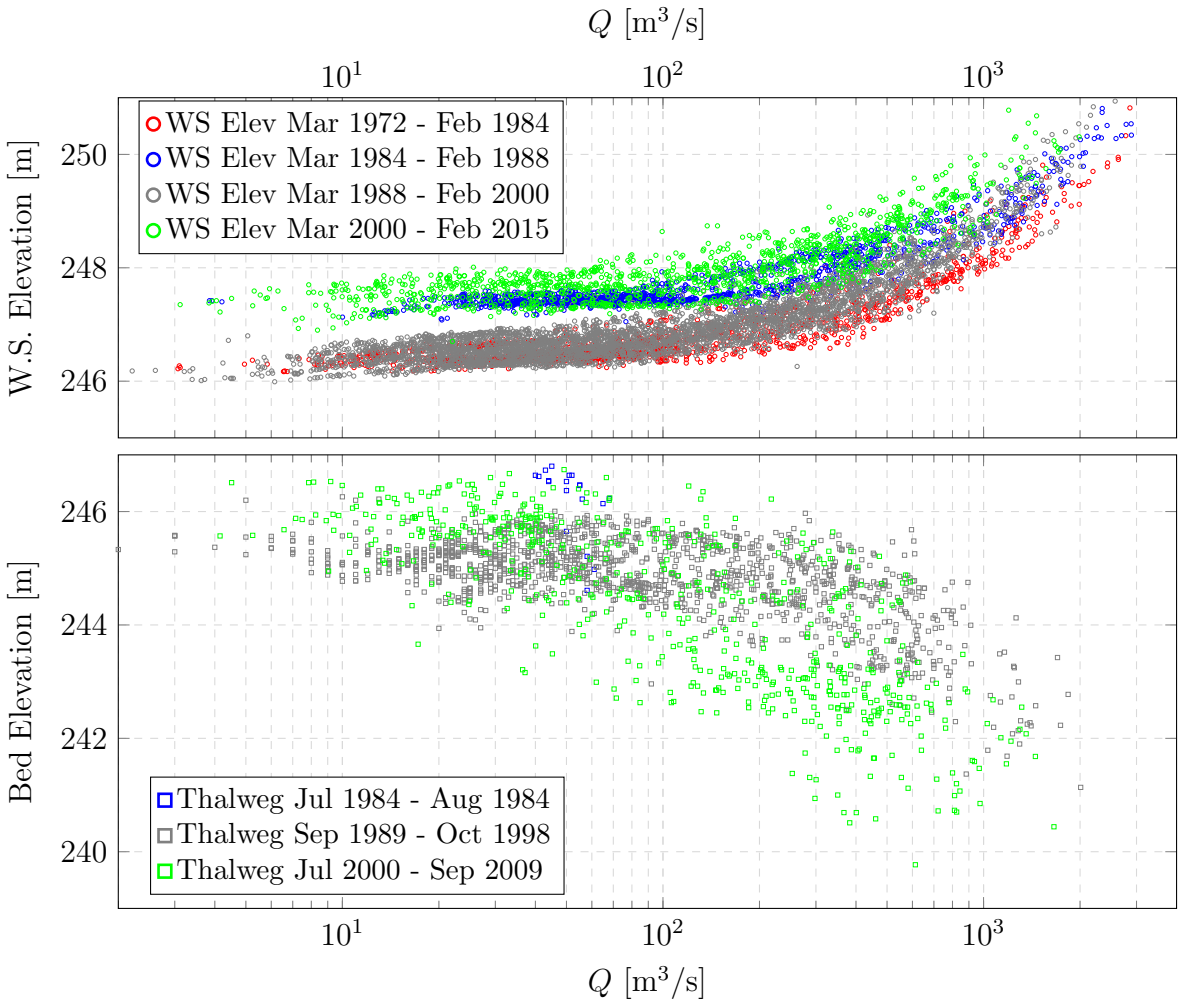


Figure 3.5: Relationship between streamflow and a) Water surface elevation, b)Bed elevation, at La Paz Gaging station.

The water surface elevations correspond to the information obtained from the flow measurement reports spanning the period March-1972 to February-2015 with a total of 8,385 points. These reports are summaries with the basic information and do not include

cross section surveys.

Approximately 2,800 detailed reports were included on the 8,385 points data set. These detailed reports span a period from 1984 to 2015 but with discontinuities between 1985-1988 and no data available for 1999. In addition, only 2,006 points of the 2,800 were used since the remaining ones were measured following the relocation of the flow measurement section cableway in Sep-2009 (the gage remained in the same place).

As it can be seen in Figure 3.5, the water surface data was plotted as different time series. The first period goes from Mar-1972 to Feb-1974. The second period goes from Mar-1984 to Feb-1988, the third one from Mar-1988 to Feb-2000 and finally, the fourth goes from Mar-2000 to Feb-2015. Bed elevation points, filtered with the considerations mentioned above, were also plotted and separated in the same time periods of the water surface data set.

It can be seen in the figure that while the water stage increases for higher Q values, the bed elevation decreases significantly. This means that the increment of water depth for higher flows is caused both by the higher water stages and by the erosion of the river bed. Furthermore, the data shows that for discharges between 10 and 1,000 m^3/s the river bed may be eroded between 1 to 5m approximately.

The main reason for dividing the data set in time series is that it can be observed that the water surface follows different patterns in the specified periods of time. The first and the third series (red and gray) present lower water stages. The corresponding changes in the year 1984 may have been caused by the the major hydrologic event that occurred during March of that year. However, there is not enough bed elevation data in that period of time to contrast with the water stages.

The international bridge located near Misión-La Paz, (500m) downstream from the gaging station) was built in 1996. The higher elevations observed after 2000 may be related with its construction but there is not enough information to support this statement.

Figure 3.6 shows the relation between water discharge and flow area. The data were fit using a power function which presents a correlation value $R^2 = 0.96$. In the case of the

velocities, which can be seen in Figure 3.7, there is more dispersion than for the flow areas, especially at low flow rates.

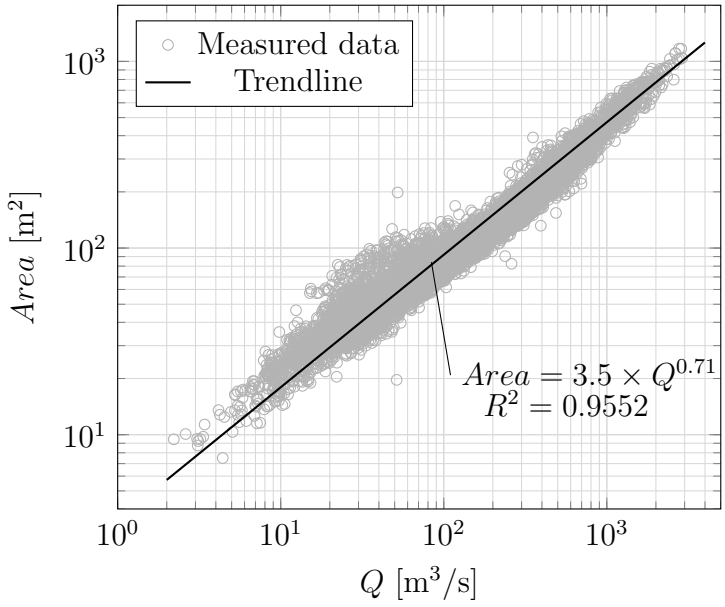


Figure 3.6: Relationship between streamflow and cross sectional area in La Paz Gaging station. Data obtained from flow measurement record's in the period between Sep-1972 and Sep-2009.

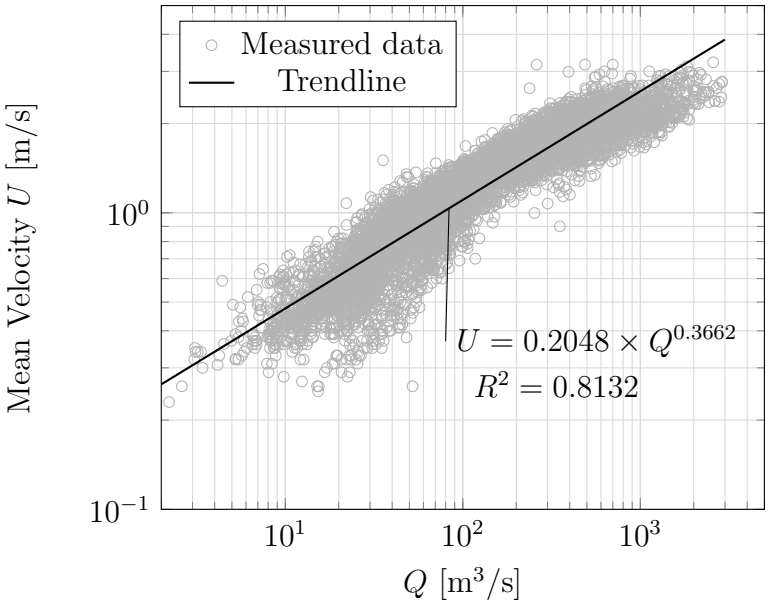


Figure 3.7: Relationship between streamflow and cross section mean velocity in La Paz Gaging station. Data obtained from flow measurement records in the period between Sep-1972 and Sep-2009.

3.1.4 Sediment Transport

Sediment rating curves were computed using the sediment load data sets measured at La Paz gaging station between 1993 and 2015. The results are shown in Figure 3.8. It can be observed that the power-law regression curve obtained for the wash-load presents a higher correlation coefficient than the coarser material. Visual inspection shows that the load fraction greater than 62μm has more dispersion, particularly for low flow rates.

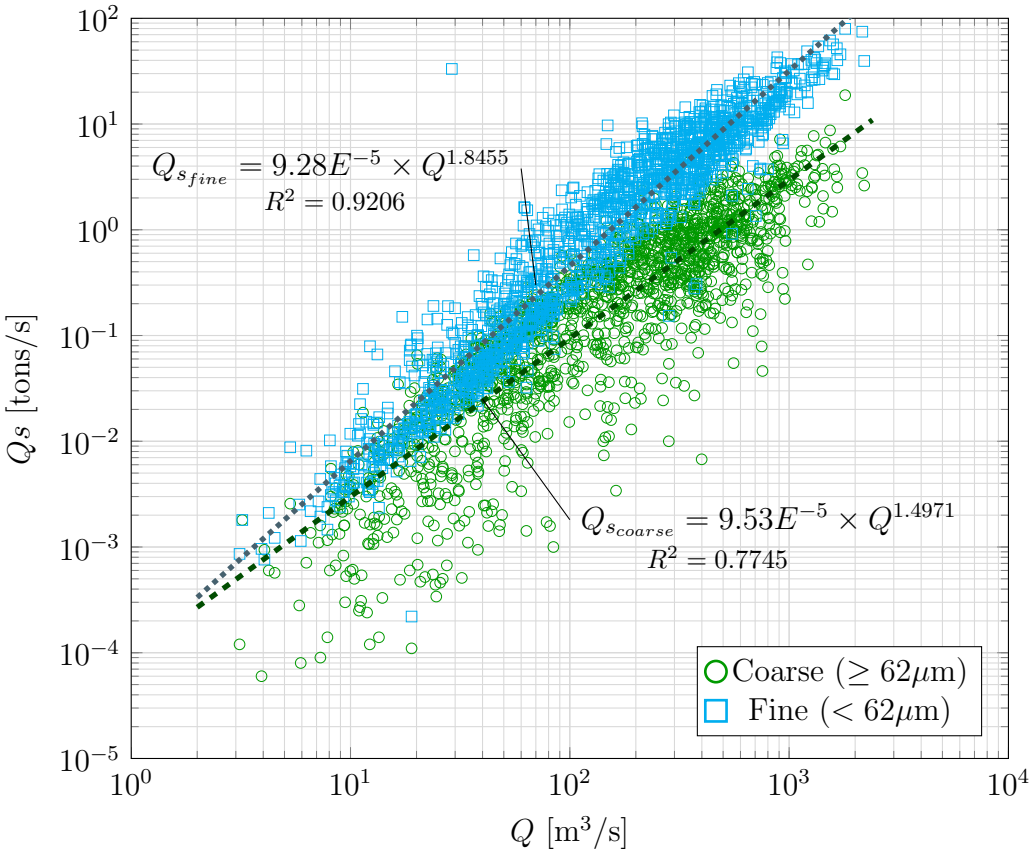


Figure 3.8: Relationship between streamflow and suspended sediment load in La Paz Gaging station. Data obtained from sediment transport measurement record's in the period between Sep-1993 and Aug-2015.

When relating the sediment load rates with the water discharge histogram of frequencies, it is possible to compute the mean annual load for the period of the data set. Then, the mean annual sediment load rate corresponds to the load rate that if maintained constant in time will produce the same annual load. These values are presented in Table 3.3. In

addition, the water discharge associated with the mean annual load rate is presented.

Table 3.3: Sediment transport annual total load and mean annual load rate.

Sediment type	Coarse	Fine	Total
Mean annual load [tons]	1.58E+07	1.65E+08	1.81E+08
Mean annual load rate $Q_{s_{mean}}$ [tons/s]	0.51	5.26	5.74
Water discharge associated with $Q_{s_{mean}}$ [m^3/s]	305.84	375.38	358.72

The analysis was made for the fine, coarse, and total sediment loads. Wash-load corresponds to 91% of the total suspended load whereas the coarser fraction represents the remaining 9%. The water discharges related to the mean suspended sediment load rates have durations of 20.6%,16.7%, and 17.61% for coarse, fine, and total fractions, respectively.

3.2 Channel-forming discharge

3.2.1 Bankfull Discharge

A cross section of the Pilcomayo River located 60m downstream from the gaging station, and surveyed in Aug-2014 is shown in Figure 3.9. Two floodplain levels can be identified. The highest floodplain has an elevation of 253m which is higher than all water stage records. Hence, it may be considered a passive floodplain. On the other hand, the lower floodplain shows an altitude close to 251m, but the top of the bench has an elevation of 251.58m. The highest stage surveyed during flow measurements is 250.9m and corresponds to a discharge of 2,574 m^3/s whereas the maximum discharge surveyed in the records was 2,892 m^3/s associated with a stage of 250.3m. These values correspond to return periods of 4.3 and 6.3 yrs, respectively (see Table 3.4 and Figure 3.4).

If considering a bankfull stage of 251m, which is the elevation of the floodplain (not the bench), the corresponding bankfull discharge will likely be between 2,500-3,000 m^3/s. These values have return periods of 4 and 7.3 yrs respectively.

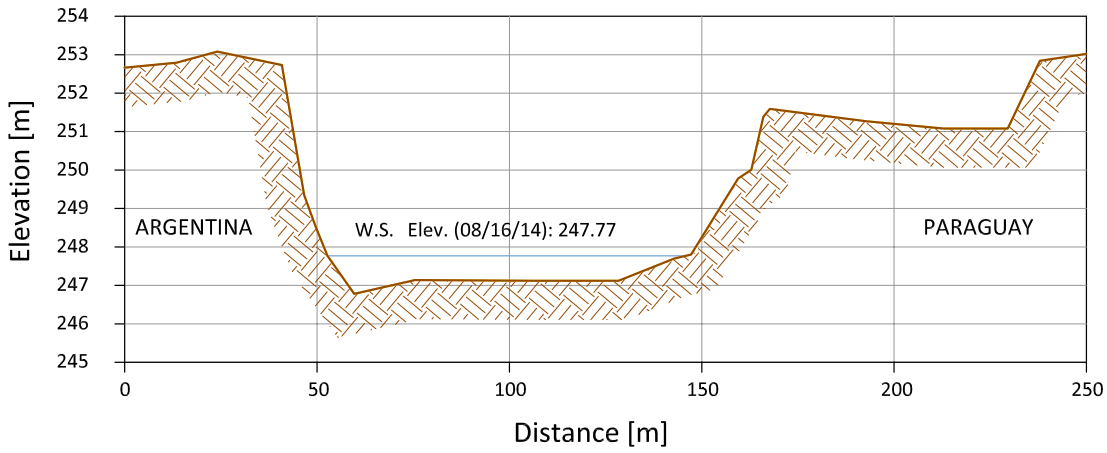


Figure 3.9: Cross section of the Pilcomayo River located 60m downstream from La Paz gaging station.

Table 3.4: Flow measurement records with highest water surface stage and maximum water flow rate measured.

Date	Q [m^3/s]	W. S. Elevation [m]	Return period [yr]
02/25/1985	2892	250.3	6.3
3/25/1999	2574	250.9	4.3

The frequency based method for determining the bankfull discharge is based on statistics of results obtained for different rivers. Soar and Thorne (2013) summarize the range of frequencies for Q_{bf} found in the literature. The authors also state that the most common return periods found are between 1 and 2 years but deviations from this range may be expected in streams with high hydrological variability. In the case of the Pilcomayo River, the recurrence intervals of 1.01 and 2 years lead to water discharges between 422 and 1,844 m^3/s. These values are lower than estimations made for the Q_{bf}] at La Paz station. Nevertheless, the Pilcomayo's hydrology presents a strong seasonality and return period values between 4 and 7.3 yrs may be justified.

Another one of the methods available in the literature for the estimation of the bankfull discharge is the analysis of the hydraulic properties of the cross sections as described in the methods. The relations between discharge Q, area A, top width W, hydraulic depth D,

and width-to-depth ratio were computed from the cross section profiles obtained from the available data. Figure 3.10 shows the results.

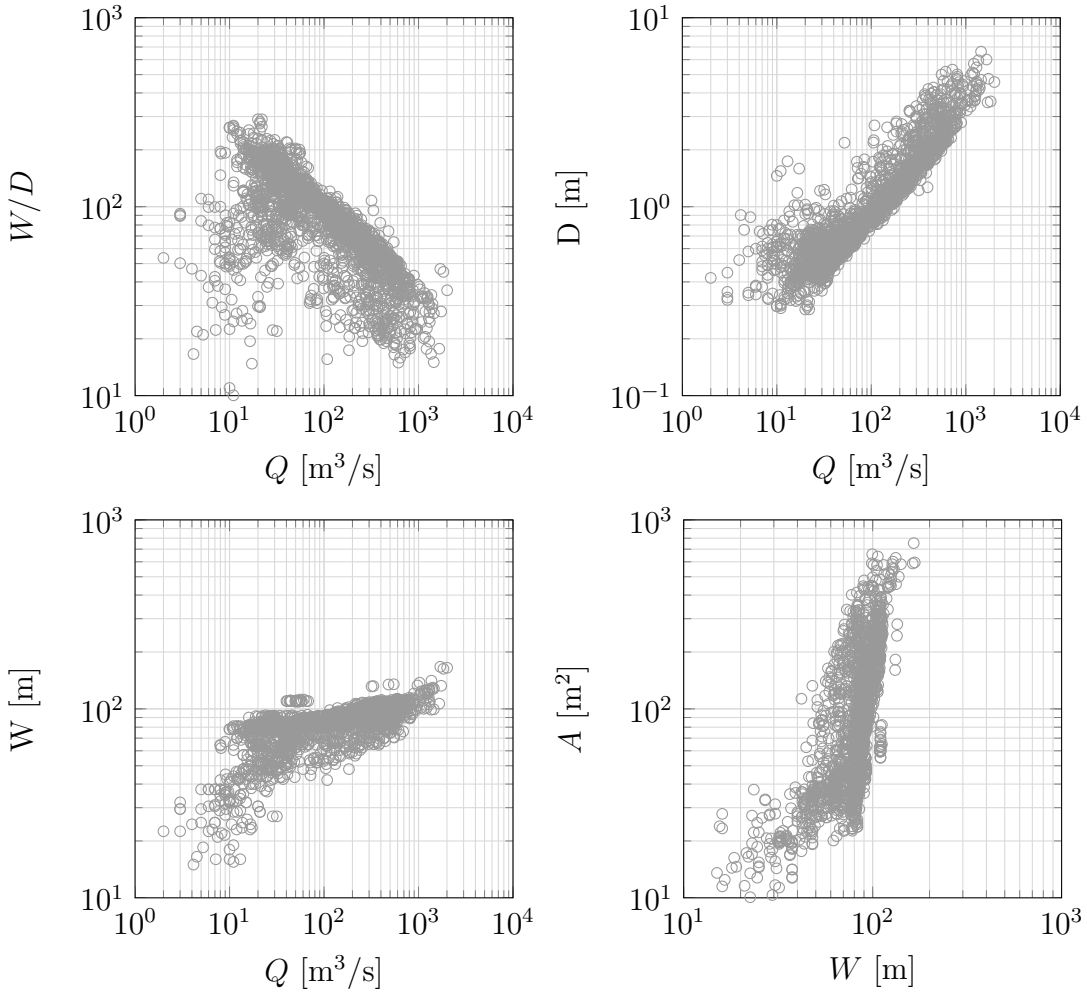


Figure 3.10: Hydraulic reelationships a) Discharge-top width W and hydraulic depth D ratio, b)Discharge- hydraulic depth D ratio, c)Discharge-top width W, d) Top width W - Area A.

The analysis was limited since the data set does not cover flow rates higher than 2,009m^3/s. Consequently the values obtained in the paragraphs above can not be verified with this method. Nevertheless, the plots show some useful information. In all the panels in Figure 3.10 there is a discontinuity for lower flow values. This behavior is due to the fact that for low discharges the stream does not cover the entire cross section. The data dispersion relates to the transition between channel shapes. For discharge values higher than 60m^3/s the data seems to follow the same pattern. In the case of the W/D ratio, it

presents a decreasing slope. No break is observed in the relation which suggests that bankfull conditions have not been reached yet. The analysis of the other three panels leads to the same conclusion.

3.2.2 Effective discharge

Effective discharge computations were made for a range of classes between 10-200. The first option was to use between 10-25 intervals, as recommended in the literature. However, all the resulting Q_{eff} values obtained were in the first interval. the reason behind this is that a significant proportion of the flows in the data series correspond to the first interval, and hence, the effective discharge may be underestimated. On the other hand, the sediment load histograms show intervals with zero frequency and a high extreme peak, even for the condition of 10 intervals. As a consequence, it was decided to decrease the interval sizes for a better representation of the frequency distribution. Best results were obtained when selecting between 40 and 60 classes, for which Q_{eff} values between 400 and 420 m^3/s were obtained. Even though intervals with zero frequency were obtained for the highest flow ranges, the histograms seemed to represent continuously the frequency distribution. The use of higher number of intervals may result in noisy histograms and show more than one peak. For these reasons, a total of 50 intervals was selected for the effective discharge computations.

It must be noted that the computations for Q_{eff} use only the transport of the coarser material only. Wash-load was not considered since theoretically this range of grain sizes does not interact with the river bed.

The results are presented in Figure 3.11. It can be seen in the water discharge histogram that even though a large number of intervals was used, 56% of the data points fall within the first interval. The resulting effective discharge has a value of $Q_{eff} = 414\mathrm{m}^3/\mathrm{s}$, and according to the flood frequency analysis, it has a recurrence interval of 1.01yrs.

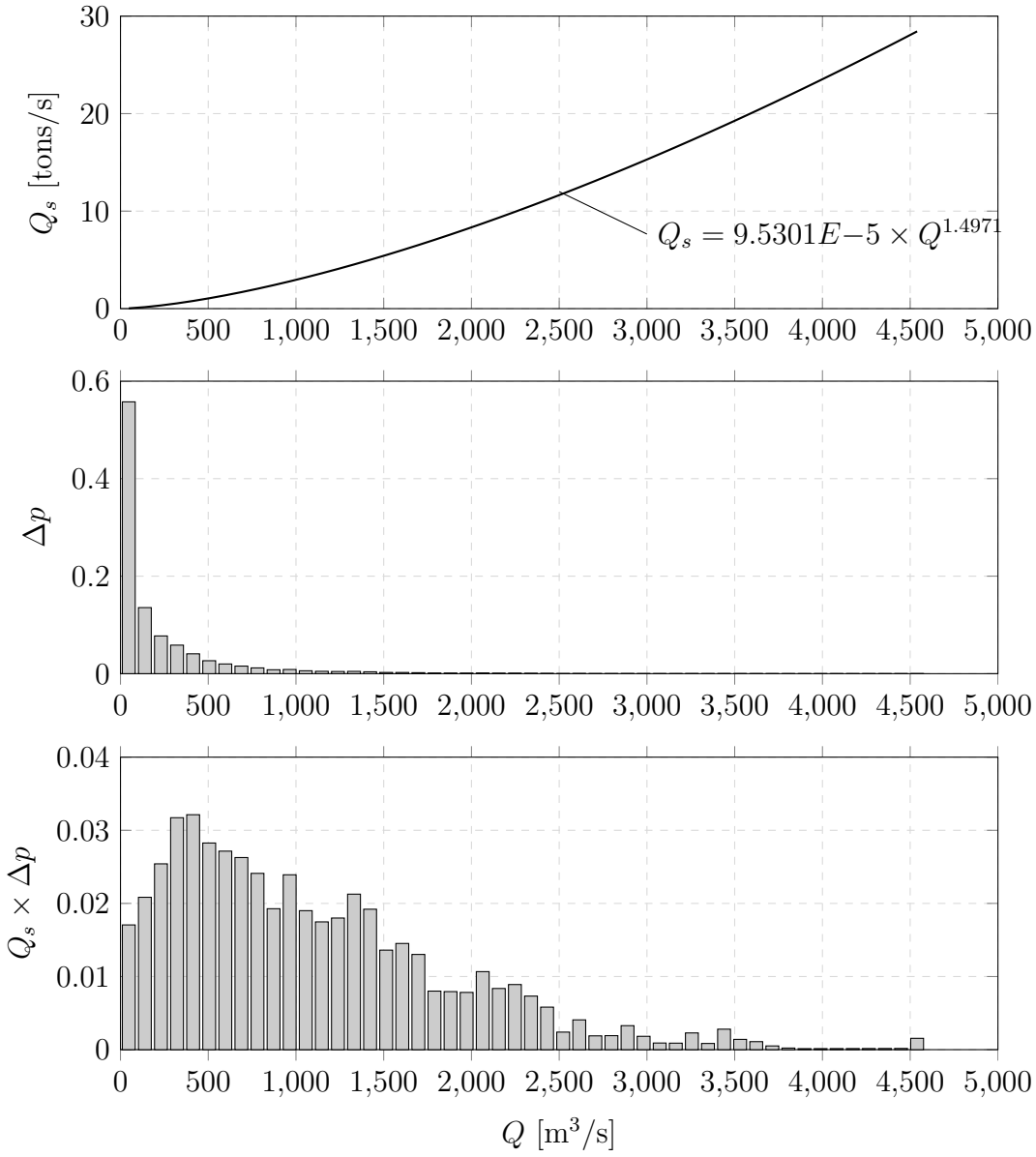


Figure 3.11: Effective discharge computation using 50 class intervals of 91.68 m^3/s each of them. Only sediment grain sizes greater than 62μm were considered. a) Sediment transpor rating curve. b) Water discharge frequency distribution. c) Sediment load frequency distribution.

Biedenharn et al. (2000) propose to check the order of magnitude of the computed effective discharge comparing its frequency of exceedance with results from other sites. Hence, the author compiled information from different streams in the U.S. and prepared a plot that relates the basin area with the duration of the effective discharge computed for each site. This chart is presented in Figure 3.12 together with the result for the Pilcomayo

River.

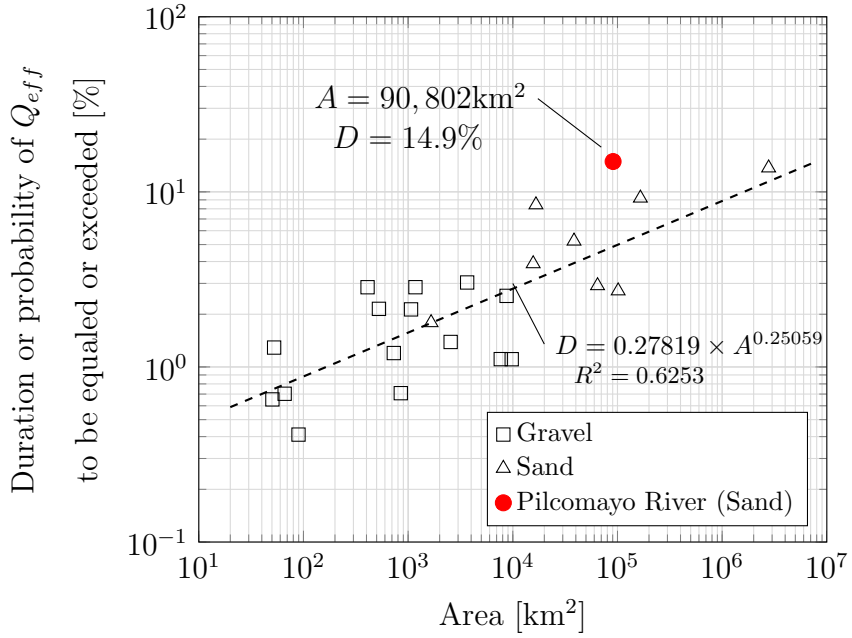


Figure 3.12: Comparison of the effective discharge probability to be equaled or exceeded for the Pilcomayo river ar Misión La Paz with data from other sites. Adopted from Biedenharn et al. (2000).

The duration of the $Q_{eff} = 414\text{m}^3/\text{s}$ at La Paz station is 14.9% (see Figure 3.3 and Table 3.1) whereas the computed basin area at the gage station is approximately 90.802km^2. It can be seen that the point is not to far away from the best-fit-line of the presented data.

3.2.3 Analysis of the Channel-Forming Discharge Results

While the estimated bankfull discharge has a magnitude between 2,500 and 3,000 m^3/s, the computed effective discharge has a value of $414\text{m}^3/\text{s}$, which is less than a fifth of these values (0.17 and 0.14 respectively). In terms of the return periods, the values of the bankfull discharge have recurrence intervals between 4 and 7yrs whereas Q_{eff} has a return period of 1.01yrs.

Since the estimation of the bankfull discharge was made by visual identification of the flood plain elevation, and by the analysis of only one cross section of the river, this estimation

may be subjective. The first reason to support this statement is that there is controversy in the definition of the bankfull stage. Herein it was defined as the altitude of the lower part of the bench, but different altitudes could have been selected. Secondly, the flow measurements data set does not cover the range of stages above 250.5m increasing the uncertainty in the bankfull flow estimations.

The highest values in the data set used for the analysis of the hydraulic properties are on the order of 2,000m^3/s. Consequently, it was not possible to analyze the behavior of the hydraulic variables in the range of bankfull discharges found previously. However, the computed relations revealed that up to the highest values in the data set, no changes or brakes were observed in the variables' behavior. This may indicate that the bankfull discharge is higher than 2,000m^3/s.

Due to the high variability of the river channel's geometry along the stream, this analysis should be repeated at other cross sections located downstream and upstream in order to reduce the uncertainties of the analysis. Furthermore, the availability of flow measurements at high stages could help complete the lack of data for analysis of the hydraulic properties of the cross section.

On the other hand, the estimation of the effective discharge is assessed by a more objective computation procedure. However, the obtained value presents a recurrence interval that is located on the lowest boundary of the return periods reported in the literature (Biedenharn et al., 2000). According to Soar and Thorne (2013), rivers with high hydrologic variability are prone to show effective discharges with lower frequencies of occurrence than perennial streams with regular regimes. Nevertheless, the sediment load histogram computed for the Pilcomayo River is well defined and the result is clear. Moreover, the order of magnitude of Q_{eff} is in agreement with the data presented by Biedenharn et al. (2000), in terms of the catchment surface and the effective discharge duration.

Both bankfull and effective discharge have the purpose of estimating the channel-forming discharge. Although Q_{bf} and Q_{eff} tend to match in rivers that are in regime, they tend to

differ in streams with high variability. According to site examinations conducted by Soar and Thorne (2013), the effective discharge was found to be lower than the bankfull discharge in 86% of the cases analyzed. Nevertheless, the obtained values of the effective discharge and the bankfull discharge may be seen as the boundaries of the range at which the true channel-forming discharge is located.

3.3 River Meander Migration Modeling

The analysis of the river paths obtained from LANDSAT images present some interesting results. The 28 centerlines are plotted in Figure 3.13where the dates matching each centerline are indicated. Great variability of the channel centerline locations can be observed, even for short periods of time. There is a tendency of the river to change its path regularly by means of cutoffs and also by recovering old river scars. Another aspect to note is the change in sinuosity between upstream and downstream of Misión La Paz. While a stream length of about 2.5km in the reach where the bridge was built seems to be stable, the upper part presents high mobility and sinuosity. On the other hand, just downstream of Misión La Paz the flow is nearly straight with high stability.

Calibration of RVR Meander was conducted by adjusting the migration coefficient in order to represent the observed migration rate from the images. The best results were obtained with a migration coefficient of 8×10^{-6}. The rest of the variables used in the model were:

- $Q_{eff} = 414\text{m}^3/\text{s}$
- W = 150m - In Figure 3.10, chart c), the range of widths for this discharge value is in the order of W=100m. However, this is on of the narrower parts of the stream and consequently, it was decided to increase it by 50m.
- Valley slope of 0.0003.

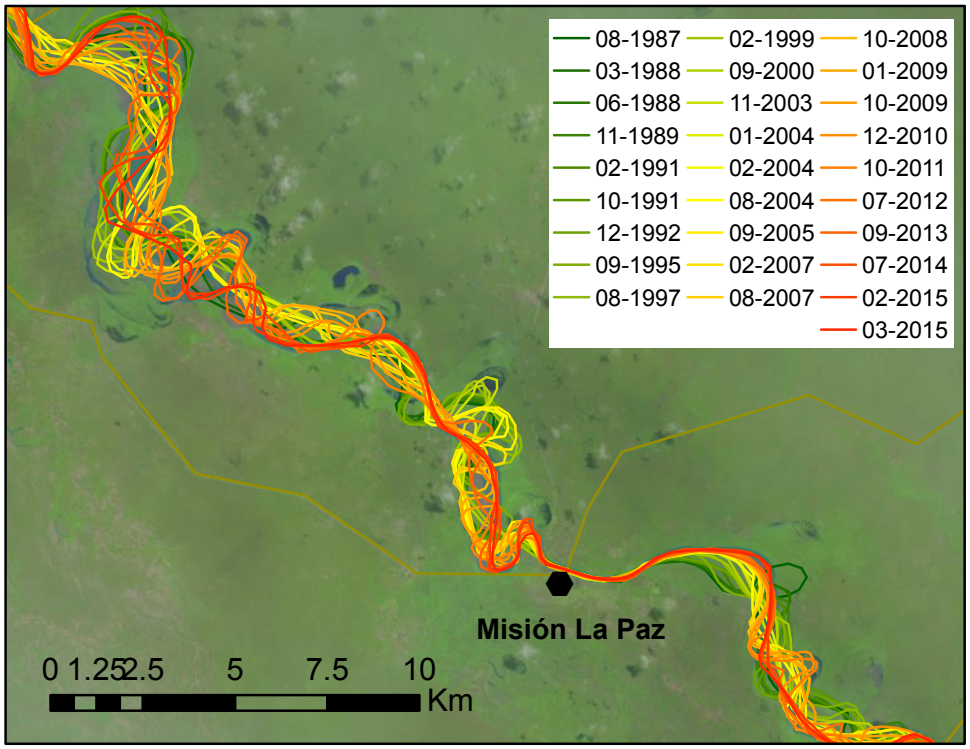


Figure 3.13: Pilcomayo River paths in the area of Misión La Paz. The river centerlines range between Aug-1987 and Mar-2015.

- Manning coefficient of 0.025. Barbagelata (2010) used Manning's values between 0.025 and 0.03.

- Scour factor of 4. This was already discussed earlier in the methods section.

Figure 3.13 shows one of the results from the calibration. It can be seen that the model does not follow the migration rates of the river. However, it can also be seen that during the 5yrs period modeled, a cutoff occurred that changed the river's planform geometry. Since the intentions behind the modeling effort were to avoid calibrating for other variables besides the migration coefficient, this result provides the best adjustment. It is remarked that the river presents predominant mechanisms of bank and stream displacement which are not necessarily those modeled by RVR Meander. During the wet season, the river varies its path by avulsions, by recovering old river scars or by chute cutoffs.

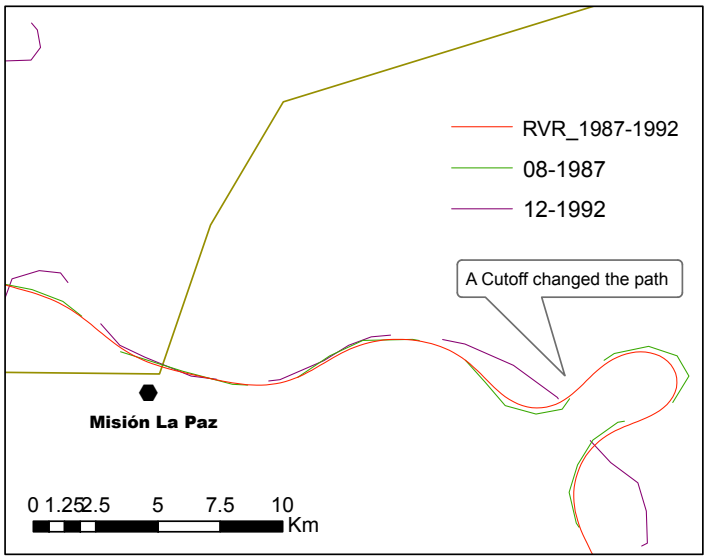


Figure 3.14: Results of the migration coefficient calibration.

Figure 3.15 shows the planform evolution for a period of 20yrs beginning on Mar-2015. Since the model initially uses a parametric function to make the path smoother, it can be observed that small meanders are sometimes smoothed out. This issue lowers the local curvature values, leading to decreased bank erosion in these regions. The dependence of near-bank velocities, thus erosion rates on curvature is the reason why in areas of high curvature, RVR Meander computes higher erosion rates.

Plotting all the RVR Meander results together allows delimiting a region over which the river stream would migrate in the future. However, the obtained planforms show lower sinuosity and meander amplitudes than the values observed from the images. Figure 3.16 presents the planforms computed with the model over the river path digitized from the images. It is observed that the model tends to achieve a stream more regular in terms of the meander wavelengths and amplitudes. Nevertheless, it is surprising that both the model and the natural stream remain stable in the reach by the bridge.

Key aspects to note from the model results are the following: First, the natural stream presents higher mobility not just because of the bank erosion process *per se* but also because of mechanisms such as avulsions, old meander path recovery, or meander cutoffs. Second, the

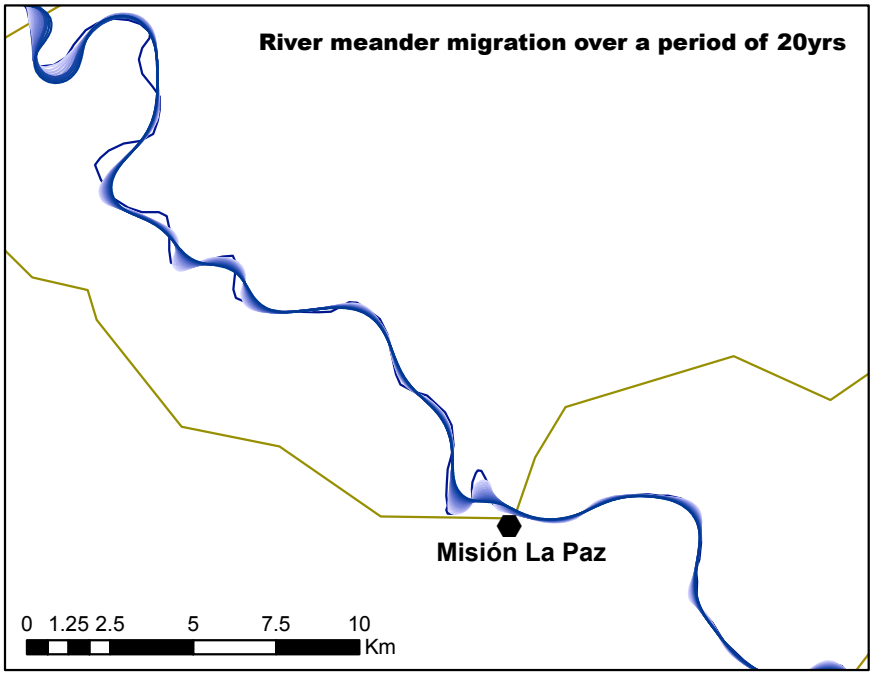


Figure 3.15: Results of the river migration during a period of 20yrs. Initial river planform corresponds to Mar-2015.

river has an inherent hydrologic variability as well as erodible bed material. These factors were found to introduce uncertainties in the applicability of the concept of channel-forming discharge (Biedenharn et al., 2000; Soar & Thorne, 2013). Consequently, the idea of a morphological discharge to model a stream with the characteristics of the Pilcomayo River may not be applicable and the results should be analyzed thoroughly.

On the other hand, the RVR Meander toolbox presents limitations produced by assumptions made in the theories behind it. The river width varies along the stream and this is not taken into account. Furthermore, the migration coefficient methodology does not take into account physical processes inherent to margin bank erosion. For instance, the possibility of wegetation along the banks which could limit the amount of erosion and thus, channel migration.

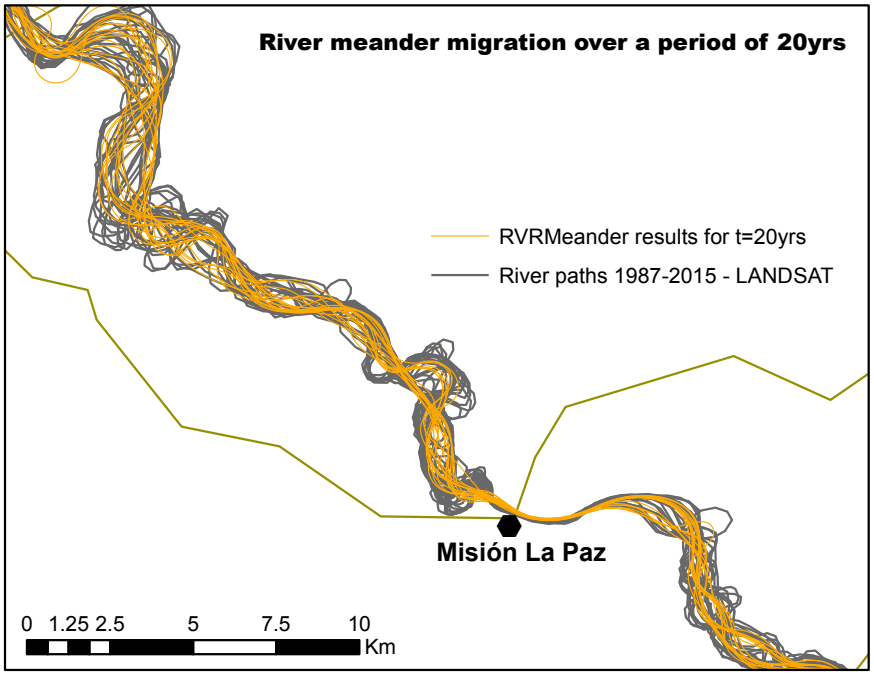


Figure 3.16: All river planforms after modeling a period of 20yrs with RVR Meander and natural planforms from 1989-2015.

Chapter 4

Conclusions

The Pilcomayo River flows over a vast alluvial fan and the bed material is susceptible to be eroded since it varies between fine and very fine sands. The hydrologic regime presents a marked seasonality, with high flows during summer and low flows in winter. The river transports large amounts of sediment that are mostly in the range of silt and clay. The hydraulic analysis of the flow measurement's cross section at Misión La Paz revealed that the bed elevation in this area is scoured 1m to 5m during floods but recovers its elevation once the flood wave passes.

Two different methods were applied to assess the channel-forming discharge at Misión La Paz. First, analysis of a channel cross section that includes the floodplain was used to determine the water discharge associated with the active floodplain elevation obtaining a value between 2,500 and 3,000m^3/s. The return periods of these water flows are 4 and 7.3 years respectively. Due to the hydrologic variability of the stream, the order of magnitude may be justified, but further analysis should be conducted with the aim of reducing the uncertainties introduced by the subjectivity in the definition of the bankfull stage. Second, the effective discharge was computed as the second method applied for the estimation of the channel-forming discharge. The resulting flow rate has a value of $414m^3/s$ whereas its recurrence interval is 1.01yrs. The bankfull and effective discharge show a marked difference. Although, a high level of uncertainty envolves the bankfull discharge computed, there are studies that argue that rivers with strong seasonality and with fine bed material result in lower values of effective discharges in relation to the bankfull values. Finally, a 2D analytical model was calibrated with the aim of predicting the river meander planform migration in

the Pilcomayo River. The migration coefficient method could not represent the spatial evolution of the Pilcomayo River planform. Reasons assumed for these results are that the main stream and bank displacement mechanisms are the recovery of meander scars as well as the occurrence of cutoffs. Investigation of the physical mechanisms of bank erosion in the Pilcomayo River would give some insight for better understanding of the river and would provide much needed input for the development of river meander migration models.

References

Abad, J. D., & García, M. H. (2006). {RVR} meander: A toolbox for re-meandering of channelized streams. *Computers & Geosciences*, *32*(1), 92 - 101. Retrieved from http://www.sciencedirect.com/science/article/pii/S0098300405001147 doi: http://dx.doi.org/10.1016/j.cageo.2005.05.006

Ackers, P., & Charlton, F. (1970). Meander geometry arising from varying flows. *Journal of Hydrology*, *11*(3), 230 - 252. Retrieved from http://www.sciencedirect.com/science/article/pii/0022169470900648 doi: http://dx.doi.org/10.1016/0022-1694(70)90064-8

Andrews, E. (1980). Effective and bankfull discharges of streams in the yampa river basin, colorado and wyoming. *Journal of Hydrology*, *46*(3-4), 311-330. doi: doi:10.1016/0022-1694(80)90084-0

Barbagelata, E. (2010). *Estudios hidrológicos, hidráulicos y fluvio-morfológicos para el río pilcomayo en la zona que comprende la estación de aforo de misión la paz, argentina* (Tech. Rep.). Comisión Trinacional para el Desarrollo de la Cuenca del Río Pilcomayo.

Benson, M. A., & Thomas, D. M. (1966). A definition of dominant discharge. *International Association of Scientific Hydrology. Bulletin*, *11*(2), 76-80. Retrieved from http://dx.doi.org/10.1080/02626666609493460 doi: 10.1080/02626666609493460

Biedenharn, D. S., Copeland, R. R., Thorne, C. R., Soar, P. J., & Hey, R. D. (2000). *Effective discharge calculation: A practical guide* (Tech. Rep.). Engineer Research and Development Center,Coastal and Hydraulics Laboratory, Vicksburg, MS.

Biedenharn, D. S., Watson, C. C., & Thorne, C. R. (2008). Sedimentation engineering. In M. H. García (Ed.), (p. 355-386). ASCE.

Carling, P. (1988). The concept of dominant discharge applied to two gravel-bed streams in relation to channel stability thresholds. *Earth Surface Processes and Landforms*, *13*(4), 355–367. Retrieved from http://dx.doi.org/10.1002/esp.3290130407 doi: 10.1002/esp.3290130407

Chow, V. T. (1988). *Applied hydrology.* McGraw-Hill Book Company, Inc; New York.

CTRP. (2015). *Monitoreo y centro de datos.* Dirección Ejecutiva de la Comisión Trinacional para el Desarrollo de la Cuenca del Río Pilcomayo. Retrieved from http://www.pilcomayo.net

Davis, D. H. (1908, Nov. - Dec.). A study of river meanders on the middle rouge. *The Journal of Geology*, *16*(8), 755-764.

Dunne, T., & Leopold, L. B. (1978). *Water in environmental planning.* Macmillan.

Gandolfo, J. S. (1940). *Estimacion de la evolucion del alveo de los rios* (Tech. Rep.). Universidad Nacional de La Plata.

Garcia, M. H., Bittner, L. D., & Nino, Y. (1994). *Mathematical modeling of meandering streams in illinois: A tool for stream management and engineering (hes 43)* (Tech. Rep.). Illinois Water Resources Center (USGS Project 04 Contract 14-08-0004-G2017. Retrieved from http://hdl.handle.net/2142/12238

Gumbel, E. (1958). *Statistics of extremes*. Columbia University Press.

Harman, C., Stewardson, M., & DeRose, R. (2008). Variability and uncertainty in reach bankfull hydraulic geometry. *Journal of Hydrology*, *351*, 13-25. Retrieved from http://www.sciencedirect.com/science/article/pii/S0022169407006695 doi: http://dx.doi.org/10.1016/j.jhydrol.2007.11.015

Ikeda, S., Parker, G., & Sawai, K. (1981, 11). Bend theory of river meanders. part 1. linear development. *Journal of Fluid Mechanics*, *112*, 363–377. Retrieved from http://journals.cambridge.org/article_S0022112081000451 doi: 10.1017/S0022112081000451

Inglis, C. C., & Lacey, G. (1947). Meanders and their bearing on river training. *The Institution of Civil Engineers Engineering Division Papers*, *5*(17), 3-24. Retrieved from http://www.icevirtuallibrary.com/doi/abs/10.1680/idivp.1947.13075 doi: 10.1680/idivp.1947.13075

Johannesson, H., & Parker, G. (1989). Velocity redistribution in meandering rivers. *Journal of Hydraulic Engineering*, *115*(8), 1019-1039. Retrieved from http://dx.doi.org/10.1061/(ASCE)0733-9429(1989)115:8(1019) doi: 10.1061/(ASCE)0733-9429(1989)115:8(1019)

Johnson, P. A., & Heil, T. M. (1996). Uncertainty in estimating bankfull conditions. *JAWRA Journal of the American Water Resources Association*, *32*(6), 1283–1291. Retrieved from http://dx.doi.org/10.1111/j.1752-1688.1996.tb03497.x doi: 10.1111/j.1752-1688.1996.tb03497.x

Knighton, D. (1998). *Fluvial forms and processes: A new perspective*. Arnold.

Leopold, L. B., Wolman, M. G., & Miller, J. P. (1964). *Fluvial processes in geomorphology*. Dover Publications. Retrieved from http://app.knovel.com/hotlink/toc/id:kpFPG00007/fluvial-processes-in/fluvial-processes-in

Martín-Vide, J., Amarilla, M., & Zárate, F. (2014). Collapse of the pilcomayo river. *Geomorphology*, *205*, 155 - 163. Retrieved from http://www.sciencedirect.com/science/article/pii/S0169555X12005569 (Discontinuities in Fluvial Systems) doi: http://dx.doi.org/10.1016/j.geomorph.2012.12.007

Motta, D. (2013). *Meander migration with physically-based bank erosion* (Doctoral dissertation, University of Illinois at Urbana-Champaign). Retrieved from http://hdl.handle.net/2142/45476

Nash, D. B. (1994). Effective sediment-transporting discharge from magnitude-frequency analysis. *The Journal of Geology*, *102*(1), 79-95. Retrieved from http://www.jstor.org/stable/30065712

Nixon, M. (1959). A study of the bank-full discharges of rivers in england and wales. *Proceedings of the Institution of Civil Engineers*, *12*(2), 157-174. Retrieved from http://www.icevirtuallibrary.com/doi/abs/10.1680/iicep.1959.12123 doi:

10.1680/iicep.1959.12123

Odgaard, A. J. (1981). Transverse bed slope in alluvial channel bends. *Journal of the Hydraulics Division*, *107*(HY12), 1677-1694.

Orfeo, O. (2007). *Dinámica sedimentológicaica del río pilcomayo (misión la paz, prov. de salta, argentina)* (Tech. Rep.). Subsecretaría de Recursos Hídricos.

Schaffernak, F. (1922). Neue grundlagen för die berechnung der geschiebeführung in flußläufen. *Leipzig und Wien, Franz Deuticke*.

Sholtes, J. S., & Bledsoe, B. P. (2016). Half-yield discharge: Process-based predictor of bankfull discharge. *Journal of Hydraulic Engineering*, *142*(8), 04016017. Retrieved from http://dx.doi.org/10.1061/(ASCE)HY.1943-7900.0001137 doi: 10.1061/(ASCE)HY.1943-7900.0001137

Soar, P. J., & Thorne, C. R. (2001). *Channel restoration design for meandering rivers* (Tech. Rep.). DTIC Document.

Soar, P. J., & Thorne, C. R. (2013). Design discharge for river restoration. In *Stream restoration in dynamic fluvial systems* (pp. 123–149). American Geophysical Union. Retrieved from http://dx.doi.org/10.1029/2010GM001009 doi: 10.1029/2010GM001009

SSRH. (2015). *Base de datos hidrológica integrada.* Subsecretaría de Recursos Hídricos de la República Argentina . Retrieved from www.hidricosargentina.gov.ar/sistema_sistema.php

Thomson, J. (1876). On the origin of windings of rivers in alluvial plains, with remarks on the flow of water round bends in pipes. *Proceedings of the Royal Society of London*, *25*(171-178), 5-8. Retrieved from http://rspl.royalsocietypublishing.org/content/25/171-178/5.short doi: 10.1098/rspl.1876.0004

USGS. (2012, October). *Shuttle radar topography mission - void filled - 3 arc-seconds (90 meters).* Retrieved from http://earthexplorer.usgs.gov/

Williams, G. P. (1978). Bank-full discharge of rivers. *Water Resources Research*, *14*(6), 1141–1154. Retrieved from http://dx.doi.org/10.1029/WR014i006p01141 doi: 10.1029/WR014i006p01141

Wolman, M. G. (1955). *The natural channel of brandywine creek, pennsylvania* (Geological survey professional paper No. 271). USGS.

Wolman, M. G., & Miller, J. P. (1960). Magnitude and frequency of forces in geomorphic processes. *The Journal of Geology*, *68*(1), 54-74. Retrieved from http://dx.doi.org/10.1086/626637 doi: 10.1086/626637

Zimmerman, C., & Kennedy, J. F. (1978). Transverse bed slopes in curved alluvial streams. *Journal of the Hydraulics Division*, *104*(ASCE 13482 Proceeding).

Zolezzi, G., & Seminara, G. (2001). Downstream and upstream influence in river meandering. part 2. planimetric development. *Journal of Fluid Mechanics*, *438*, 183–211.